**Electronic Supplementary Information**

for

# 2,2'-Biimidazole Contained Conjugated Polymer—A Novel Fluorescent Sensing Platform

Yinyin Bao, Qianbiao Li, Bin Liu, Fanfan Du, Jiao Tian, Hu Wang, Yanxue Wang and Ruke Bai*

*CAS Key Laboratory of Soft Matter Chemistry, Department of Polymer Science and Engineering, University of Science and Technology of China, Hefei, P. R. China 230026.*

*E-mail: bairk@ustc.edu.cn*

*Tel: 0086-551-3600722; Fax: 0086-551-3631760*

## Contents

## 1. Materials and Methods.

Cationic compounds such as LiCl, NaCl, KCl, $MgCl_2$, $CaCl_2$, $FeCl_3$, $ZnCl_2$, $CdCl_2$, $NiCl_2$, $CuCl_2$, $HgCl_2$, $Mn(OAc)_2$, $Pb(OAc)_2$, $La(NO_3)_3$, and $AgNO_3$ were purchased from Shanghai Chemical Co. and used without further purification. $Et_3N$ and 1,4-Dioxane were freshly distilled over appropriate drying agents. Reactions that required oxygen-free conditions were carried out under Argon atmosphere using standard Schlenk techniques. All the other reagents were purchased and used without further purification.

Fluorescence spectra measurements were performed on a Shimadzu RF-5301PC spectroflurophotometer. Absorption spectra were determined on a Pgeneral UV-Vis TU-1901 Spetrophotometer. $^1H$ and $^{13}C$ NMR spectra were taken on a Bruker AVANCE Ⅱ spectrometer with TMS as an internal standard and $CDCl_3$ as solvent. Molecular weights and molecular weight distributions were determined by GPC equipped with a Waters 1515 pump, a Waters 2414 RI detector, and Waters UV/RI detectors (set at 30 °C). It used a series of three linear Styragel columns HR3, HR4, and HR6 at an oven temperature of 45 °C. MS were performed on a ProteomeX-LTQ spectrometer. FT-IR spectra were taken on a Bruker EQUINOX55 spectrometer. All spectra were recorded at room temperature (temperature controlled at 25 ± 3 $^oC$).

## 2. Synthesis and characterization.

Synthesis of (**M0**)

2,2'-Biimidazole (2.68 g, 0.02 mol) was dispersed in DMF (120 mL), and 1.0 N NaOH(aq) (2.5 ml) was added. The suspension was stirred and heated to 50℃. A solution composed of *n*-butyl acrylate (5.12g, 0.04 mol) solubilized in DMF (10 mL) was added dropwise. After 4 h, the solution was neutralized with aqueous hydrochloric acid and heating discontinued. The solvent was removed by rotary evaporation and the product was purified by recrystallization from methanol to give **M0** (4.71 g) as red solid, yield: 81%. $^1H$ NMR (400 MHz, CDCl3): δ= 7.07(d, 4H), 4.75(t, 4H), 4.06(t, 4H), 2.89(t, 4H), 1.57(m, 4H), 1.34(m, 4H), 0.91(t, 6H). $^{13}C$ NMR (100 MHz, CDCl3): δ= 171.5, 137.8, 127.9, 122.1, 64.6, 43.5, 35.9, 30.5, 19.1, 13.6.

MS: *m/z* =390.28.

Synthesis of (**M1**)

*N*-Bromosuccinimide (2.6 g, 14.6 mmol) was added to a chloroform solution (20 mL) of **M0** (2.8 g, 7.2 mmol) under vigorous stirring under air. After 2 h, the reaction mixture was neutralized with NaOH(aq), and the product was extracted with chloroform. After being washed with water, the combined organic layers were dried ($Na_2SO_4$) and chromatographed on silica gel (petroleum ether: acetone = 20:1, v/v) to give **M1** (2.6 g) as red solid, yield: 67%. $^1$H NMR (400 MHz, CDCl3): δ= 7.10(s, 2H), 4.73(t, 4H), 4.07(t, 4H), 2.86(t, 4H), 1.59(m, 4H), 1.37(m, 4H), 0.93(t, 6H). $^{13}$C NMR (100 MHz, CDCl3): δ= 170.6, 138.4, 129.0, 105.8, 64.7, 42.1, 34.6, 30.5, 19.1, 13.7. MS: *m/z* =548.06.

Synthesis of (**M2**)

N-hexyl-3,6-diiodocarbazole (0.75 g, 1.5 mmol), pinacolborane (0.7 mL, 4.5 mmol), $Et_3N$ (1.25 mL, 8.5 mmol) and $PdCl_2$(dppf) (0.05 g, 0.06 mmol) were dissolved in anhydrous 1,4-dioxane (10 mL) under Ar atmosphere and the solution was stirred overnight at 90 °C. After cooling to room temperature, the mixture was poured into water (50 mL) and extracted with $Et_2O$ (3 × 20 mL). The combined organic layers were dried ($Na_2SO_4$) and chromatographed on silica gel (petroleum ether: ethyl acetate = 20:1, v/v). Then the resulting light yellow solid was purified by recrystallization from hexane to give **4** (0.33 g) as white solid, yield: 44%. $^1$H NMR (400 MHz, CDCl3): δ= 8.66(s, 2H), 7.90(d, 2H), 7.39(d, 2H), 4.30(t, 2H), 1.85(m, 2H), 1.39(s, 24H), 1.35–1.27(m, 6H), 0.84(t, 3H). $^{13}$C NMR (100 MHz, CDCl3): δ= 142.6, 131.9, 128.0, 122.8, 108.1, 83.5, 43.1, 31.5, 28.8, 26.8, 24.9, 22.5, 13.9. MS: *m/z* = 504.22.

Synthesis of (**P1**)

N-Hexyl-3,6-bis(4,4,5,5,-tetramethyl-1,3,2-dioxaborolan-2-yl)carbazole(0.20 g, 0.4 mmol), 5,5'-dibromo-N,N'-di(*n*-butyl propionato)-2,2'-biimidazole (0.22 g, 0.4

mmol), $Pd(PPh_3)_4$ (0.05 g, 0.04 mmol), and $Na_2CO_3$ (0.9 g, 8.5 mmol) were added to a flask under Ar atmosphere. A solvent mixture of toluene (8 mL), water (4 mL), and ethanol (2 mL) was degassed and added to the reaction mixture. The resulting mixture was refluxed with vigorous stirring for 48 h. After cooling to room temperature, the mixture was poured into water (30 mL) and extracted with $CHCl_3$ (3 × 30 mL). The combined organic layers were dried ($Na_2SO4$) and purified by precipitated from hexane to give **P1** (0.033 g) as slightly gray solid, yield: 13%. $^1H$ NMR (400 MHz, $CDCl_3$): δ= 8.20(s, 2H), 7.58-7.53(m, 4H), 7.21-7.18(m, 2H), 4.99-4.80(m, 4H), 4.39(t, 2H), 4.02-3.88 (m, 4H), 2.84-2.66(m, 4H), 1.97-1.95(m, 2H), 2.03-1.95 (m, 2H), 1.61-1.10 (m, 18H), 0.91-0.75(m, 9H).

Synthesis of (**P2**)

N-Hexyl-3,6-bis(4,4,5,5,-tetramethyl-1,3,2-dioxaborolan-2-yl)carbazole(0.15 g, 0.3 mmol), 5,5'-dibromo-N,N'-di(*n*-butyl propionato)-2,2'-biimidazole (0.15 g, 0.27 mmol), 4,7-dibromo-2,1,3-benzothiazole (0.009 g, 0.03 mmol), $Pd(PPh_3)_4$ (0.035 g, 0.03 mmol), and $Na_2CO_3$ (0.64 g, 6 mmol) were added to a flask under Ar atmosphere. A solvent mixture of toluene (6 mL), water (3 mL), and ethanol (1.5 mL) was degassed and added to the reaction mixture. The resulting mixture was refluxed with vigorous stirring for 48 h. After cooling to room temperature, the mixture was poured into water (30 mL) and extracted with $CHCl_3$ (3 × 30 mL). The combined organic layers were dried ($Na_2SO4$) and purified by precipitated from hexane to give **P1** (0.11 g) as slightly gray solid, yield: 60%. $^1H$ NMR (400 MHz, $CDCl_3$): δ= 8.20(s, 2H), 7.96(m, 0.2H), 7.58-7.48(m, 4H), 7.22-7.16(m, 1.8H), 4.94-4.80(m, 1.8H), 4.39(br s, 2H), 4.01-3.88 (m, 3.6H), 2.84-2.64(m, 3.6H), 1.96(br s, 2H), 1.48-1.09 (m, 6H+10.8H), 0.91-0.80(m, 3H+5.4H).

## 3. Polymerization Results.

Table S1. Polymerization Results and Characterization of **P1** and **P2**

| Polymer | $M_w$[a] | $M_n$[a] | PDI[a] | Absorbance[b] ($\lambda_{max}$, nm) | Emission[b] ($\lambda_{max}$, nm) | Quantum[c] Yield |
|---|---|---|---|---|---|---|
| P1 | 4400 | 2900 | 1.53 | 312 | 416 | 0.2 |
| P2 | 11600 | 10700 | 1.09 | 310, 450 | 416, 560 | 0.17 |

[a] Estimated from GPC (eluent: DMF, polystyrene standards). [b] All spectra were recorded in dioxane at a concentration of polymer-bound biimidazole of 8.0 μM. Emission spectra were measured with excitation at 333 nm. [c] The quantum yields of **P1** and **P2** were determined using Quinine bisulfate in 0.05 M $H_2SO_4$ solution as the standard.

## 4. Sensing Mechanism.

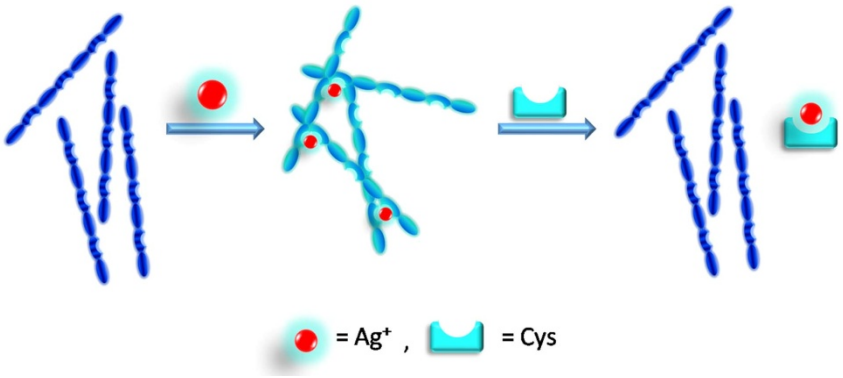


Scheme S1. Possible interaction mechanism of the polymer and $Ag^+$ and Cys

**5. Fluorometric Analysis.**

The stock solutions of **P1** and **P2** were prepared in dioxane (1.0 mM), and were diluted before use as required. The cation solutions were prepared in DMF with a concentration of 8.0 mM. The amino acids were prepared in deionized water with a concentration of 8.0 mM. The quantum yields of **P1** and **P2** were determined according to the following equation:

$$\Phi_u = \Phi_s \frac{F_u A_s n_u^2}{F_s A_u n_s^2}$$

Where Φ is quantum yield; *F* is integrated area under the corrected emission spectra; *A* is absorbance at the excitation wavelength; *n* is the refractive index of the solution; the subscripts *u* and *s* refer to the unknown and the standard, respectively. Quinine bisulfate in 0.05 M $H_2SO_4$ solution was used as the standard, which has a quantum yield of 0.55.

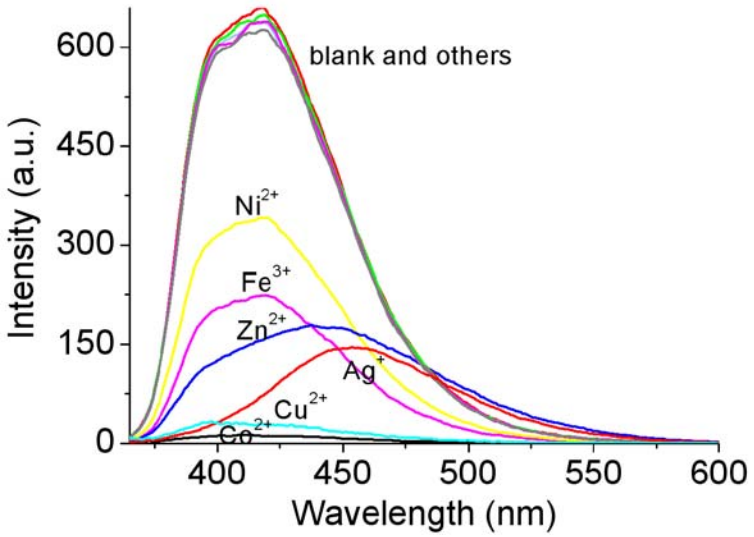


**Fig. S1** Fluorescence spectra of **P1** in the presence of various metal ions (50.0 equiv of $Na^+$, $K^+$, $Mg^{2+}$, $Ca^{2+}$, and 5.0 equiv $Li^+$, $Ag^+$, $Zn^{2+}$, $Cd^{2+}$, $Hg^{2+}$, $Ni^{2+}$, $Cu^{2+}$, $La^{3+}$, $Mn^{2+}$, $Pb^{2+}$, $Fe^{3+}$) in dioxane. [**P1**] = 8.0 μM. $\lambda_{ex}$ = 333 nm.

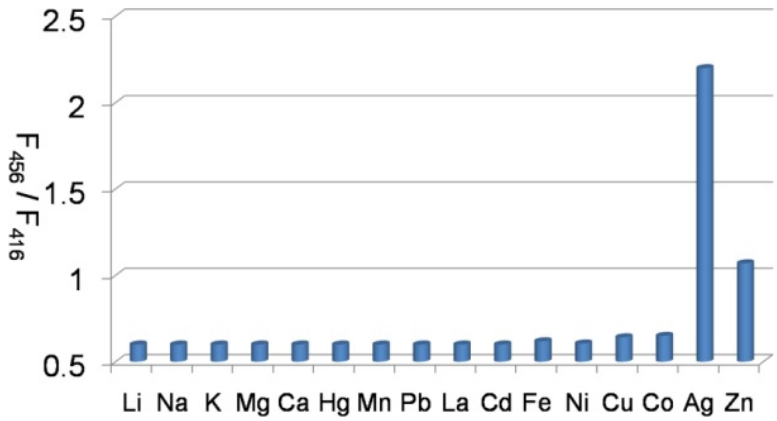


**Fig. S2** Intensity ratio $F_{560nm}/F_{416nm}$ of **P1** in the presence of indicated metal ions. [**P1**] = 8.0 μM. $\lambda_{ex}$ = 333 nm.

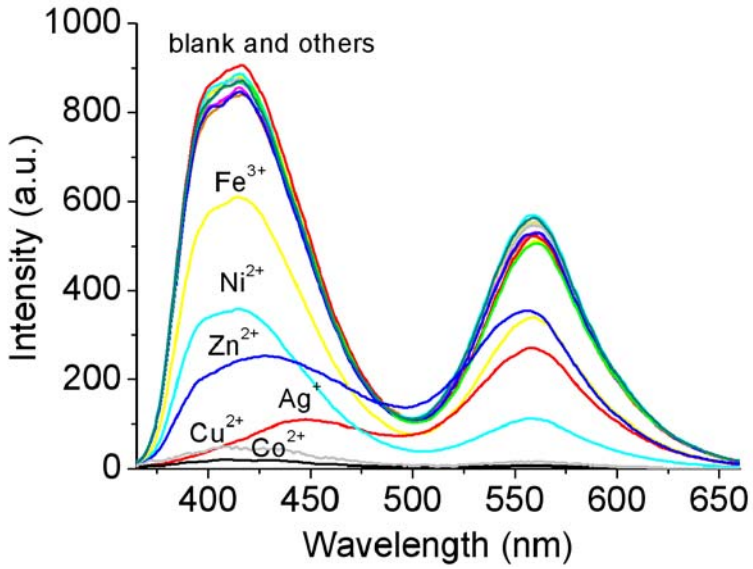


**Fig. S3** Fluorescence spectra of **P2** in the presence of various metal ions (50.0 equiv of $Na^+$, $K^+$, $Mg^{2+}$, $Ca^{2+}$, and 5.0 equiv $Li^+$, $Ag^+$, $Zn^{2+}$, $Cd^{2+}$, $Hg^{2+}$, $Ni^{2+}$, $Cu^{2+}$, $La^{3+}$, $Mn^{2+}$, $Pb^{2+}$, $Fe^{3+}$) in dioxane. [**P2**] = 8.0 μM. $\lambda_{ex}$ = 333 nm.

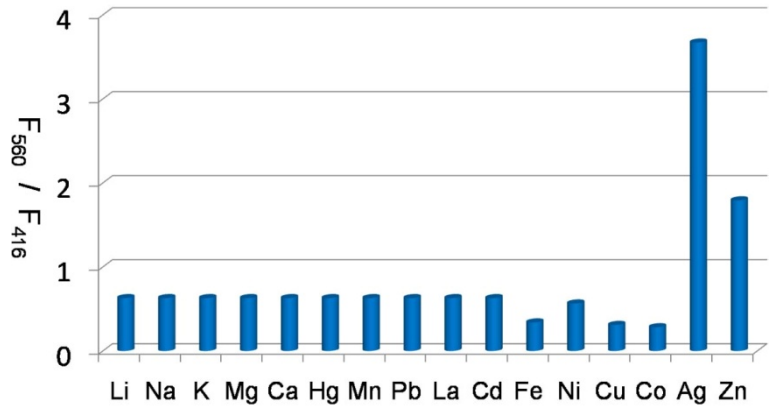


**Fig. S4** Intensity ratio $F_{560nm}/F_{416nm}$ of **P2** in the presence of indicated metal ions. [**P2**] = 8.0 μM. $\lambda_{ex}$ = 333 nm.

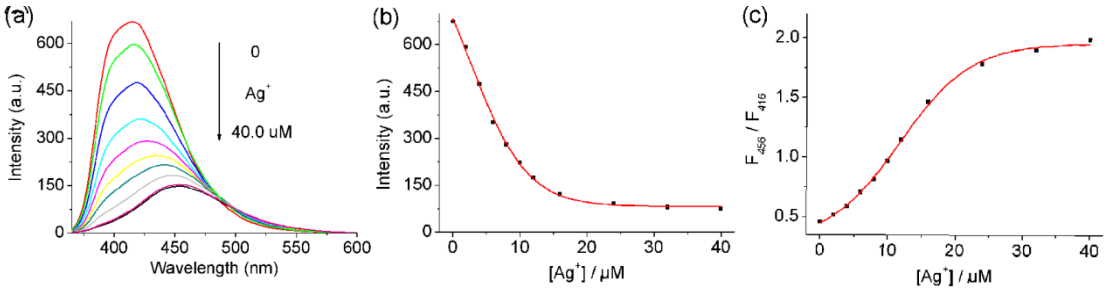


**Fig. S5** (a) Fluorescence spectra of **P1** + $AgNO_3$ in the presence of increasing $Ag^+$ concentrations. (b) Fluorescence titration profiles of **P1** with $AgNO_3$ at 416 nm. (c) Ratiometric calibration curve $F_{456nm}/F_{416nm}$ of **P1** as a function of $Ag^+$ concentration. [**P1**] = 8.0 μM. $\lambda_{ex}$ = 333 nm.

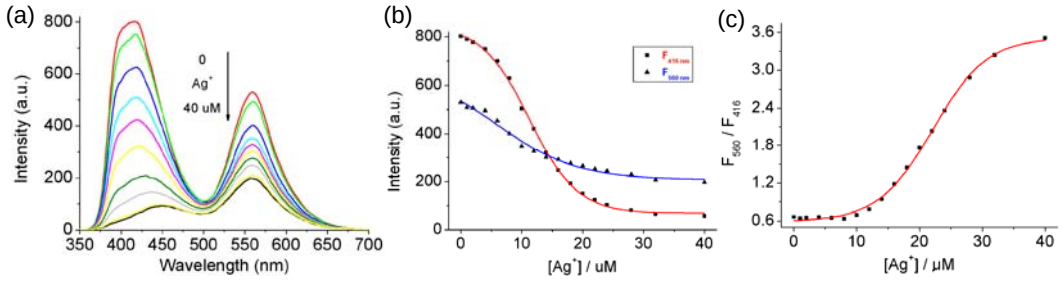


**Fig. S6** (a) Fluorescence spectra of **P2** + $AgNO_3$ in the presence of increasing $Ag^+$ concentrations. (b) Fluorescence titration profiles of **P2** with $AgNO_3$ at 416 and 560 nm. (c) Ratiometric calibration curve $F_{560nm}/F_{416nm}$ of **P2** as a function of $Ag^+$ concentration. [**P2**] = 8.0 μM. $\lambda_{ex}$ = 333 nm.

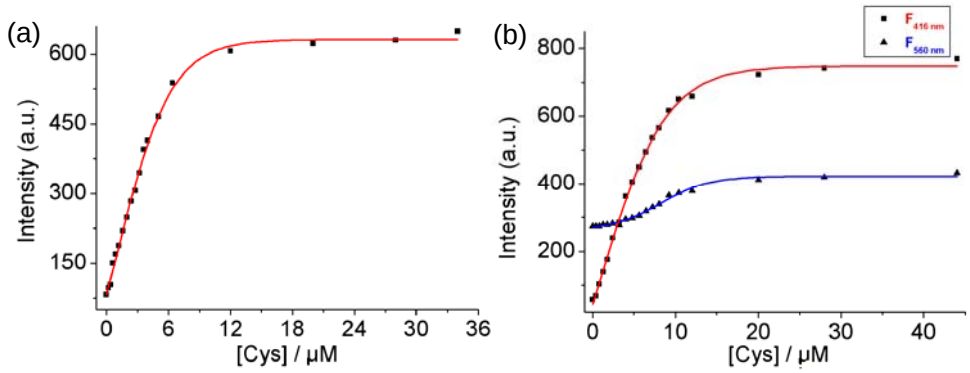


**Fig. S7** (a) Fluorescence titration profiles of **P1-Ag**$^+$ with Cys at 416 nm. (b) Fluorescence titration profiles of **P2-Ag**$^+$ with Cys at 416 and 560 nm. [**P1**] = [**P2**] = 8.0 μM. $\lambda_{ex}$ = 333 nm.

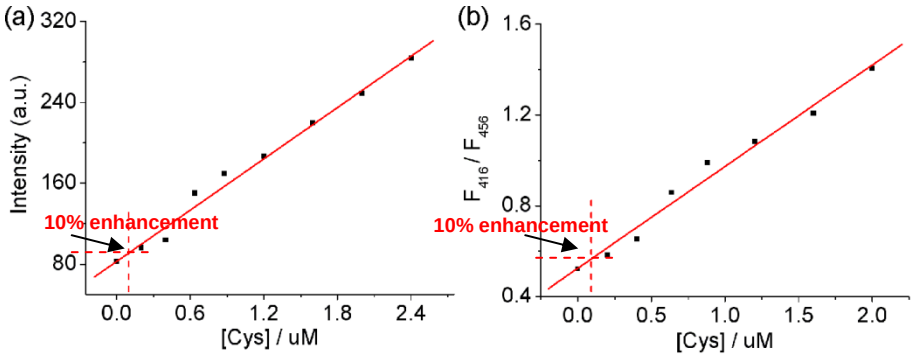


**Fig. S8**. (a) Fluorescence emission changes at 416 nm and (b) intensity ratio $F_{416nm}/F_{456nm}$ of **P1**-$Ag^+$ vs low Cys concentration. [**P1**] = 8.0 μM. $\lambda_{ex}$ = 333 nm.

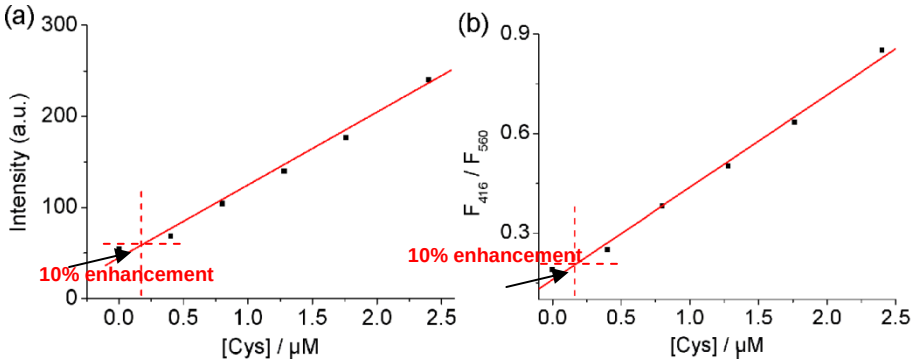


**Fig. S9**. (a) Fluorescence emission changes at 416 nm and (b) intensity ratio $F_{416nm}/F_{560nm}$ of **P2**-$Ag^+$ vs low Cys concentration. [**P2**] = 8.0 μM. $\lambda_{ex}$ = 333 nm.

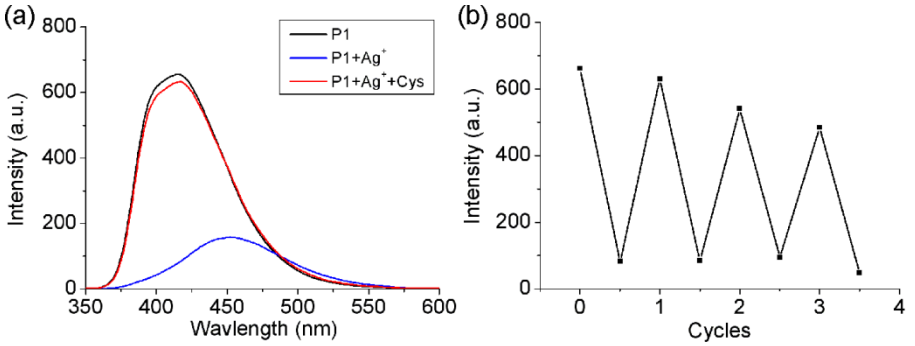


**Fig. S10.** (a) Fluorescence spectra of **P1**, **P1** + $Ag^+$ and **P1**-$Ag^+$ + Cys. (b) The fluorescence intensity of **P1** at 416 nm upon addition of $Ag^+$ and Cys.

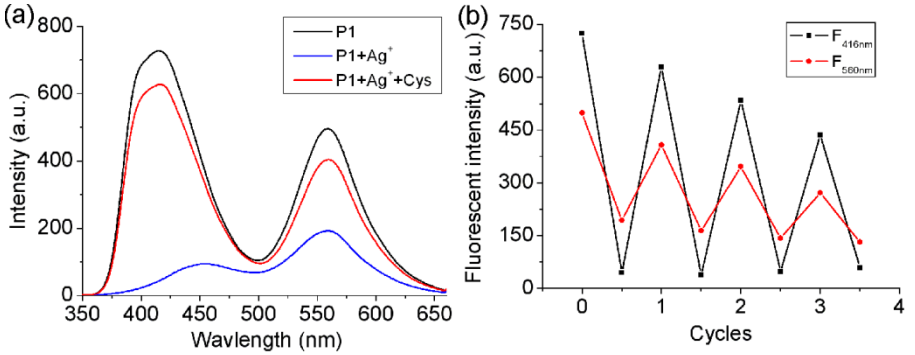


**Fig. S11.** (a) Fluorescence spectra of **P2**, **P2** + $Ag^+$ and **P2**-$Ag^+$ + Cys. (b) The fluorescence intensity of **P2** at 416 nm and 560 nm upon addition of $Ag^+$ and Cys.

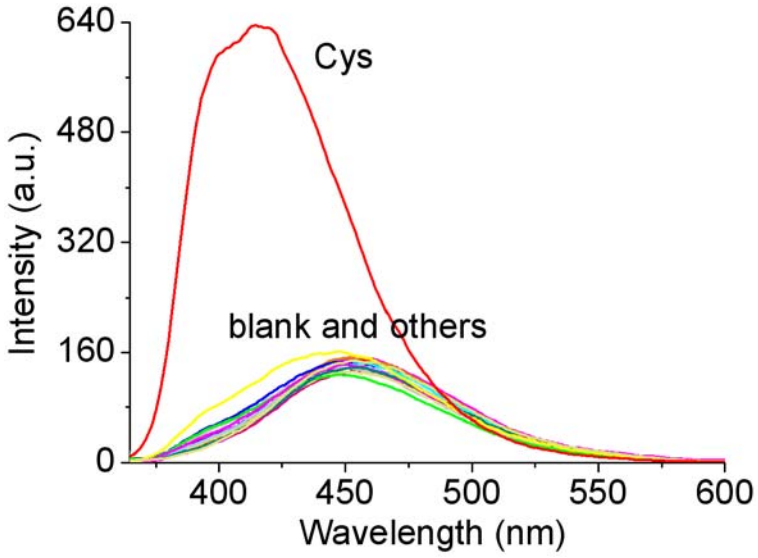


**Fig. S12** Fluorescence spectra of **P1**-$Ag^{+}$ in the presence of various amino acids. [**P1**] = 8.0 μM. $\lambda_{ex}$ = 333 nm.

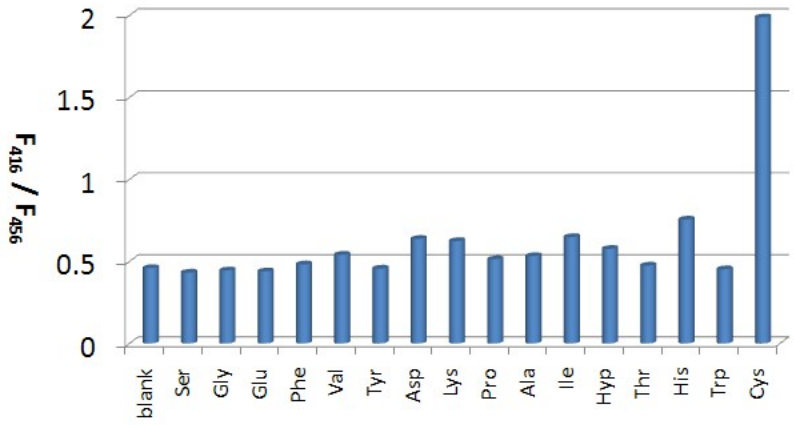


**Fig. S13** Intensity ratio $F_{416nm}/F_{456nm}$ of **P1**-$Ag^{+}$ in the presence of indicated amino acids. [**P1**] = 8.0 μM. $\lambda_{ex}$ = 333 nm.

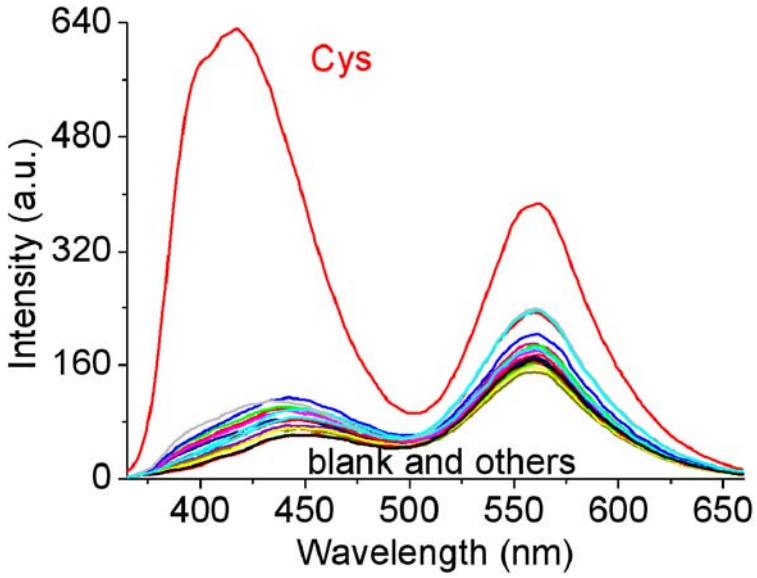


**Fig. S14** Fluorescence spectra of **P2**-$Ag^{+}$ in the presence of various amino acids. [**P2**] = 8.0 μM. $\lambda_{ex}$ = 333 nm.

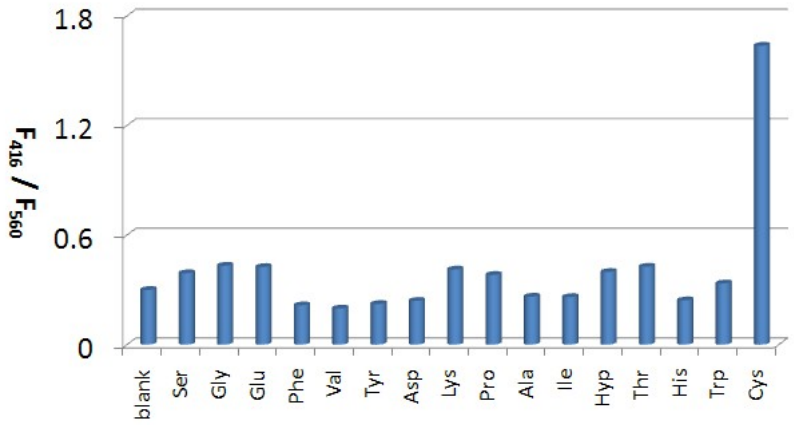


**Fig. S15** Intensity ratio $F_{416nm}/F_{560nm}$ of **P2**-$Ag^{+}$ in the presence of indicated amino acids. [**P2**] = 8.0 μM. $\lambda_{ex}$ = 333 nm.

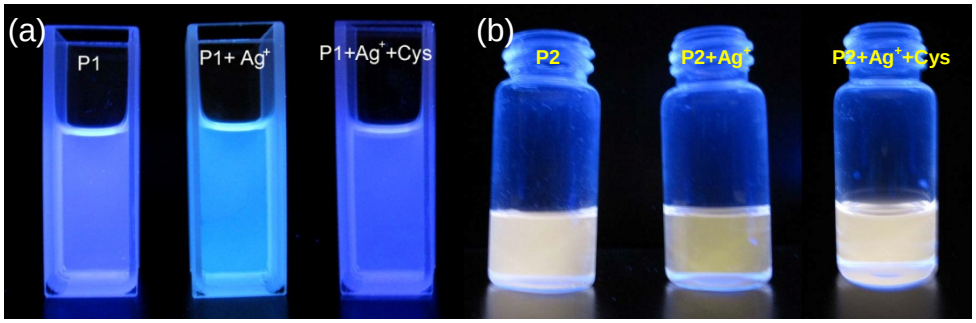


**Fig. S16** Under UV lamp fluorescent color changes observed for (a) **P1** and (b) **P2** upon addition of $Ag^{+}$ and Cys in dioxane solution. [**P1**] = [**P2**] = 8.0 μM.

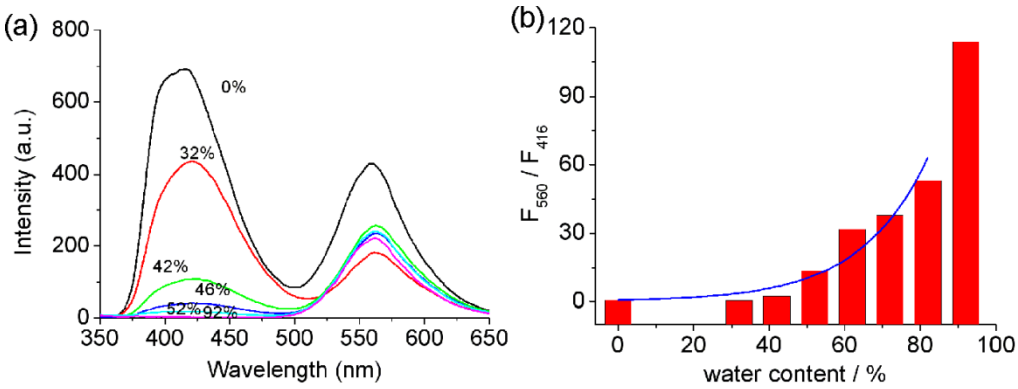


**Fig. S17** (a) Fluorescence spectra of **P2** in the presence of increasing water content. (b) Intensity ratio $F_{560nm}/F_{416nm}$ of **P2** in the presence of increasing water content. [**P2**] = 8.0 μM. $\lambda_{ex}$ = 333 nm.

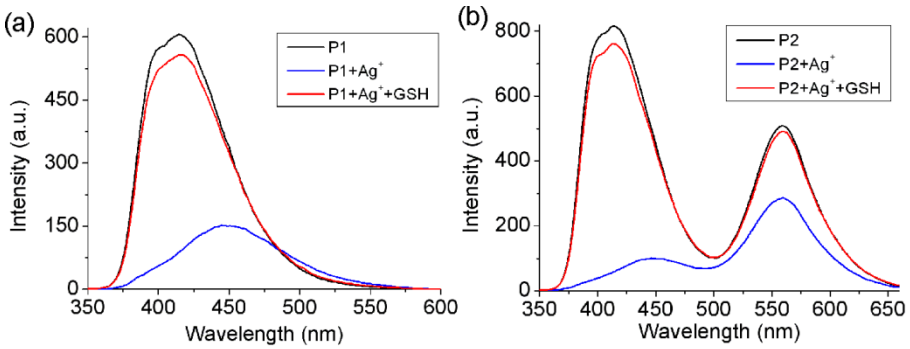


**Fig. S18.** (a) Fluorescence spectra of **P1**, **P1** + $Ag^+$ and **P1**-$Ag^+$ + GSH. (b) Fluorescence spectra of **P2**, **P2** + $Ag^+$ and **P2**-$Ag^+$ + GSH.

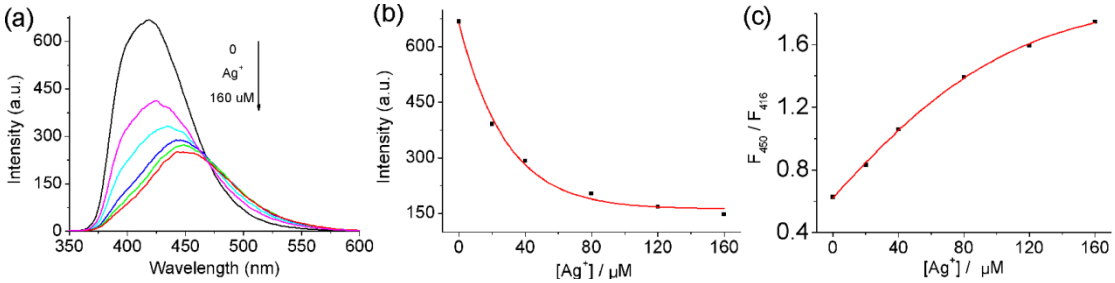


**Fig. S19** (a) Fluorescence spectra of **P1** + $AgNO_3$ in the presence of increasing $Ag^+$ concentrations in aqueous solution (*dioxane/water=9/1*). (b) Fluorescence titration profiles of **P1** with $AgNO_3$ at 416 nm. (c) Ratiometric calibration curve $F_{450nm}/F_{416nm}$ of **P1** as a function of $Ag^+$ concentration. [**P1**] = 8.0 μM. $\lambda_{ex}$ = 333 nm.

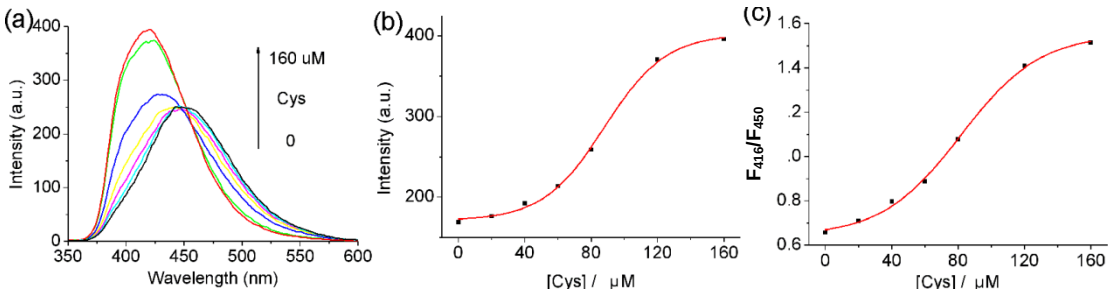


**Fig. S20** (a) Fluorescence spectra of **P1**-$Ag^{+}$ + Cys in the presence of increasing Cys concentrations in aqueous solution (*dioxane/water=9/1*). (b) Fluorescence titration profiles of **P1**-$Ag^{+}$ with Cys at 416 nm. (c) Ratiometric calibration curve $F_{416nm}/F_{450nm}$ of **P1**-$Ag^{+}$ as a function of Cys concentration. [**P1**] = 8.0 μM. $\lambda_{ex}$ = 333 nm.

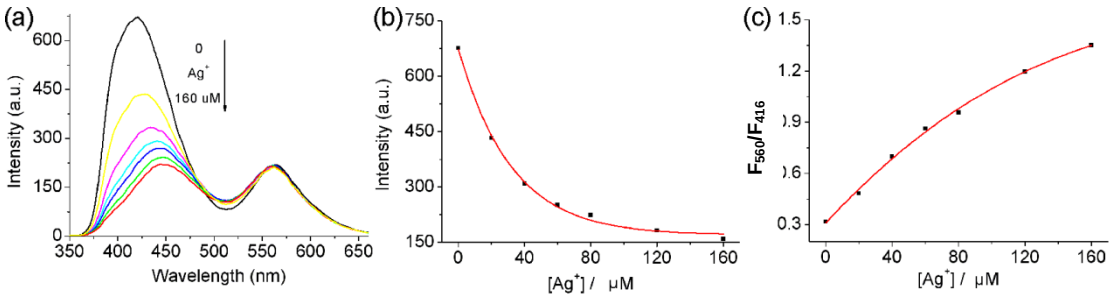


**Fig. S21** (a) Fluorescence spectra of **P2** + $AgNO_3$ in the presence of increasing $Ag^{+}$ concentrations in aqueous solution (*dioxane/water=9/1*). (b) Fluorescence titration profiles of **P2** with $AgNO_3$ at 416 nm. (c) Ratiometric calibration curve $F_{450nm}/F_{416nm}$ of **P2** as a function of $Ag^{+}$ concentration. [**P2**] = 8.0 μM. $\lambda_{ex}$ = 333 nm.

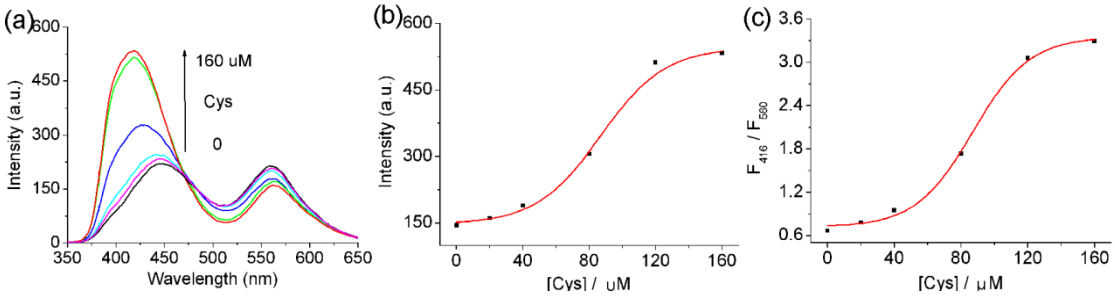


**Fig. S22** (a) Fluorescence spectra of **P2**-$Ag^{+}$ + Cys in the presence of increasing Cys concentrations in aqueous solution (*dioxane/water=9/1*). (b) Fluorescence titration profiles of **P2**-$Ag^{+}$ with Cys at 416 nm. (c) Ratiometric calibration curve $F_{416nm}/F_{450nm}$ of **P2**-$Ag^{+}$ as a function of Cys concentration. [**P2**] = 8.0 μM. $\lambda_{ex}$ = 333 nm.

## 6. UV-visible Absorbance Analysis.

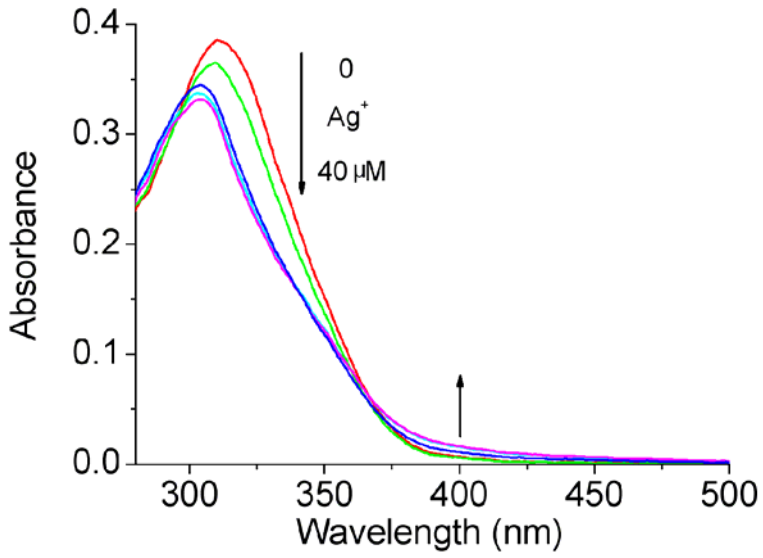


**Fig. S23** Absorbance spectra of **P1** + $AgNO_3$ in dioxane solution of increasing $Ag^+$ concentrations.

[**P1**] = 8.0 μM.

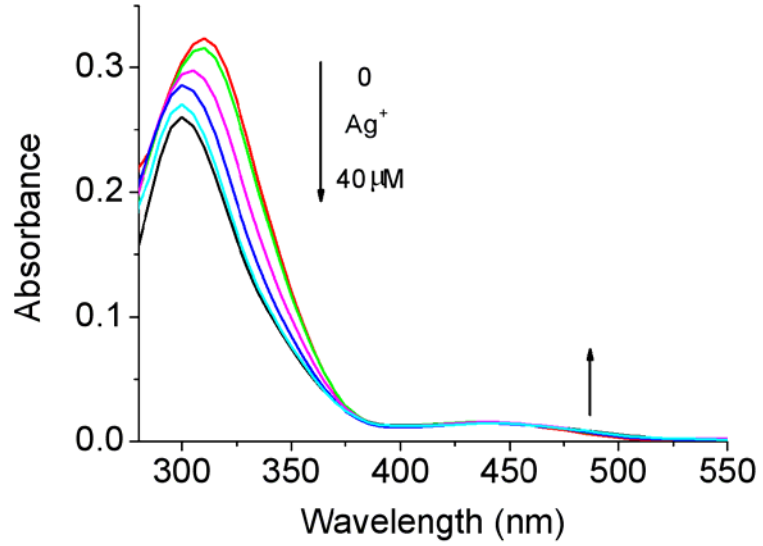


**Fig. S24** Absorbance spectra of **P2** + $AgNO_3$ in dioxane solution of increasing $Ag^+$ concentrations.

[**P2**] = 8.0 μM.

## 7. NMR Data.

$^{1}$H NMR ($CDCl_3$, 400 MHz) spectrum of **M0**

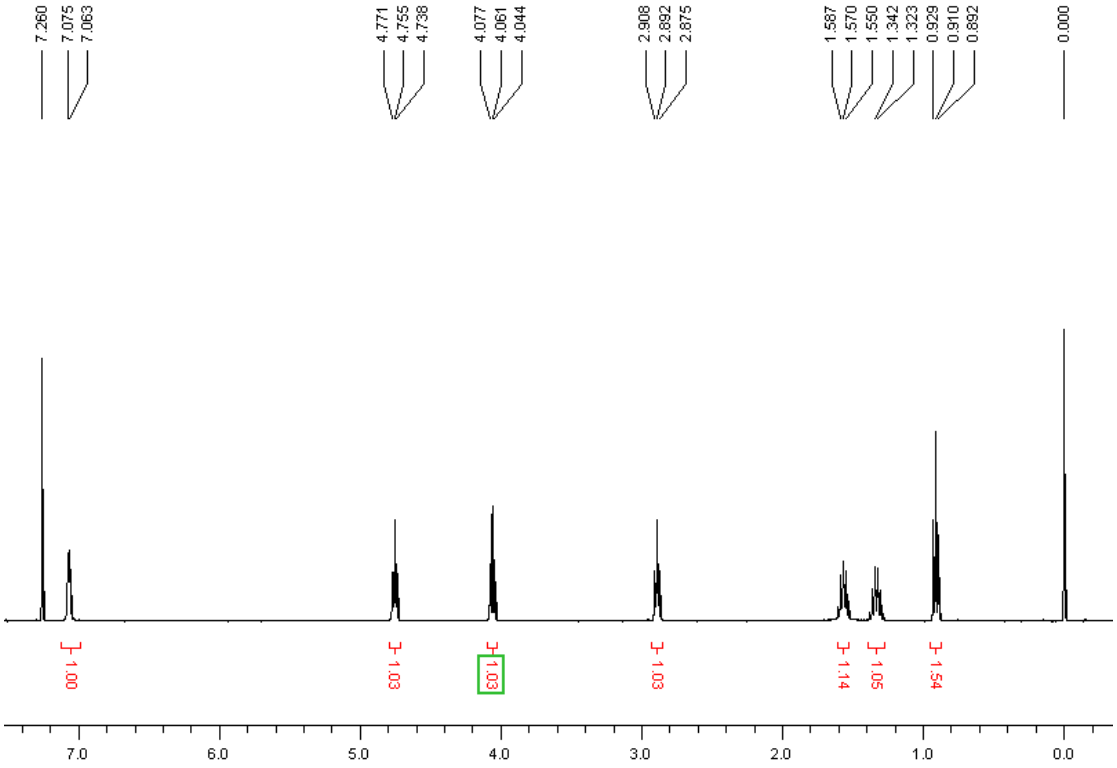


$^{13}$C NMR ($CDCl_3$, 400 MHz) spectrum of **M0**

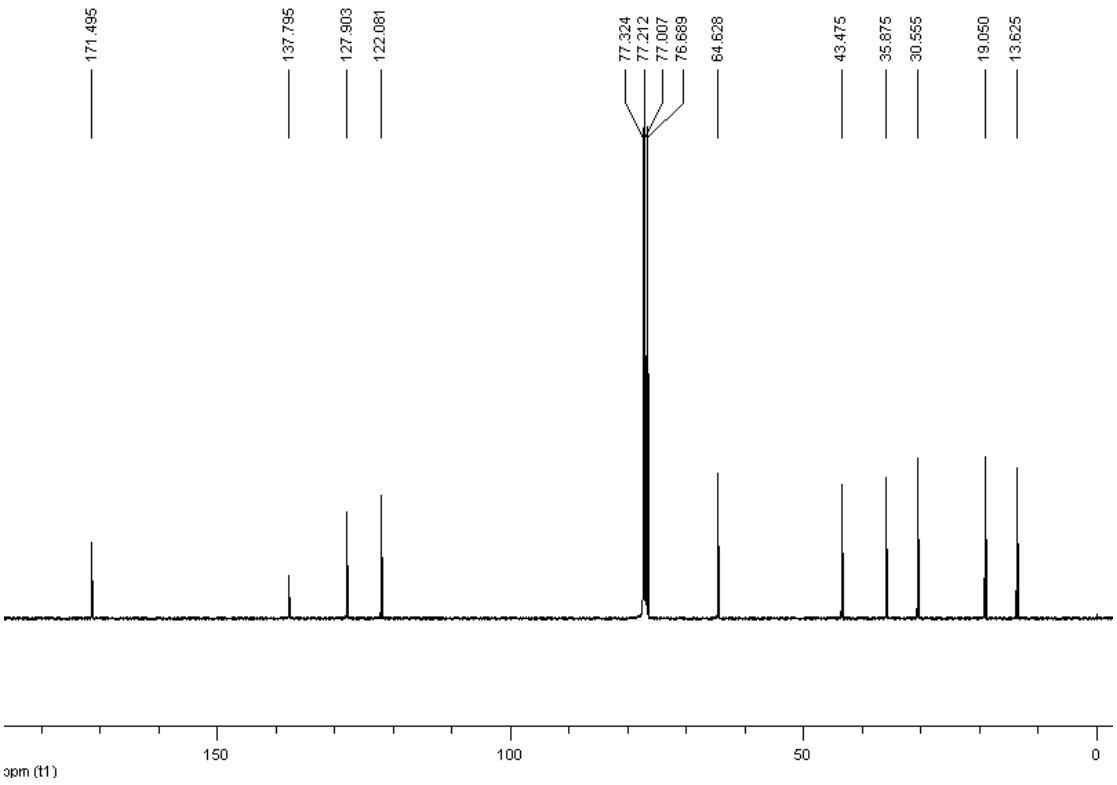

$^{1}$H NMR ($CDCl_3$, 400 MHz) spectrum of **M1**

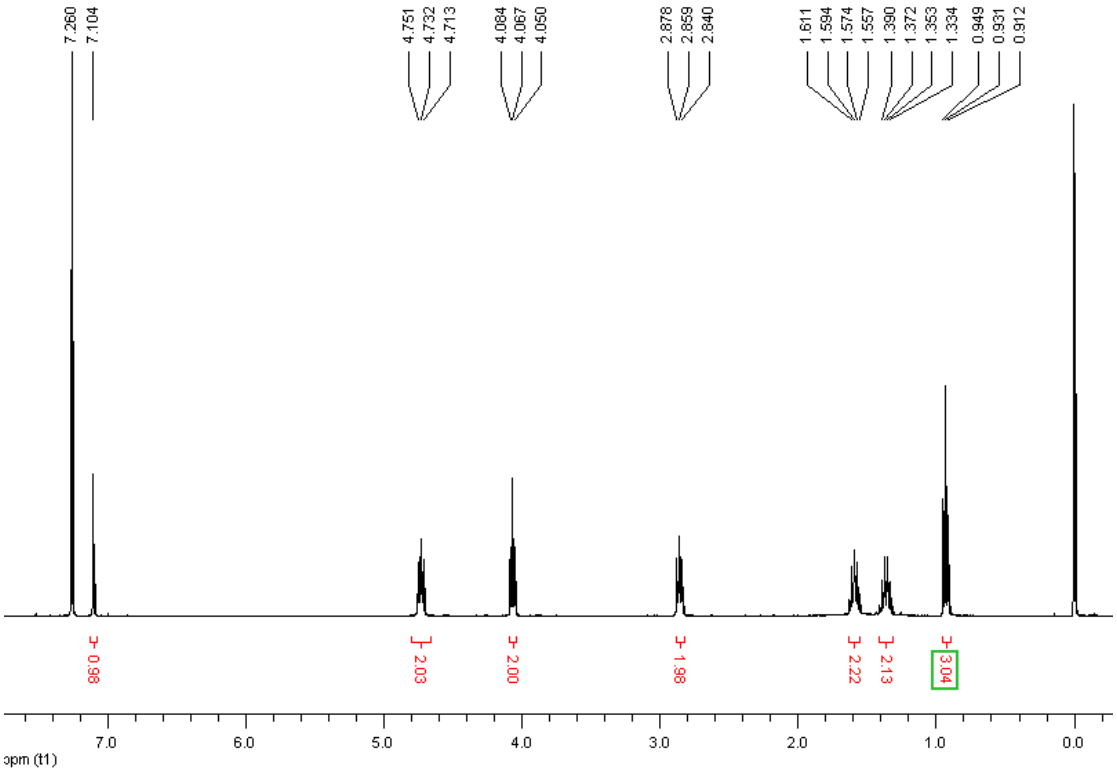


$^{13}$C NMR ($CDCl_3$, 400 MHz) spectrum of **M1**

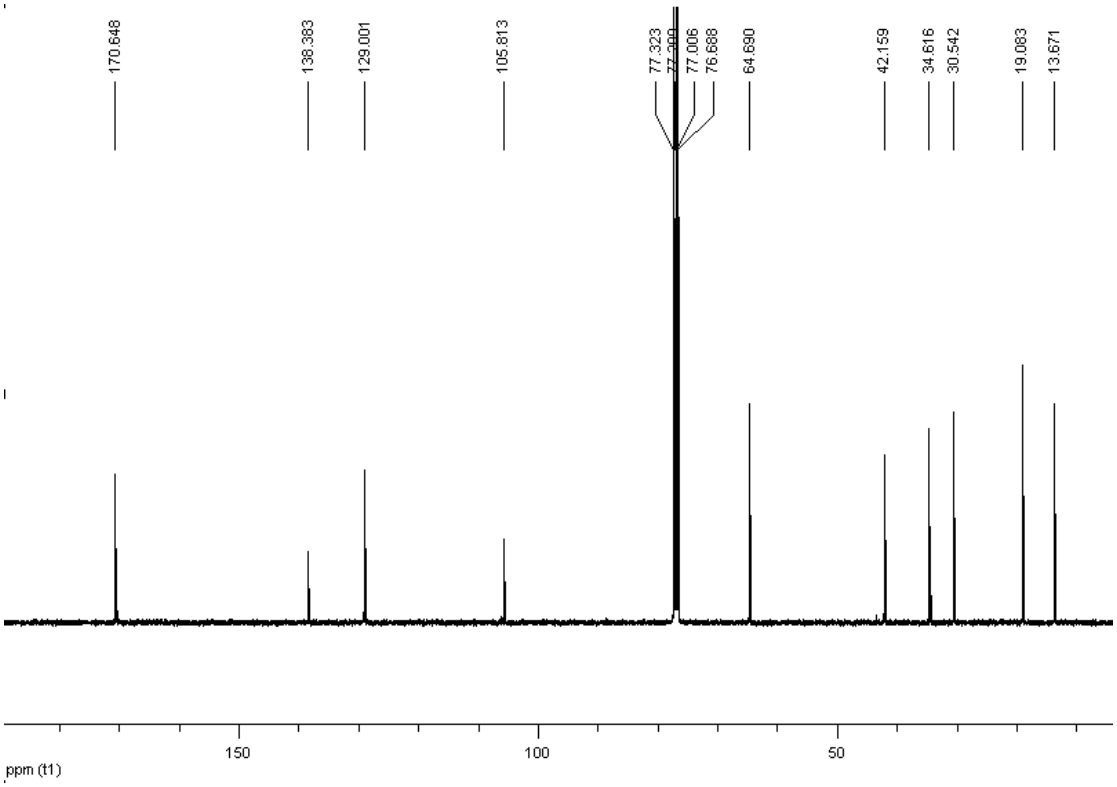

$^{1}$H NMR ($CDCl_3$, 400 MHz) spectrum of **M2**

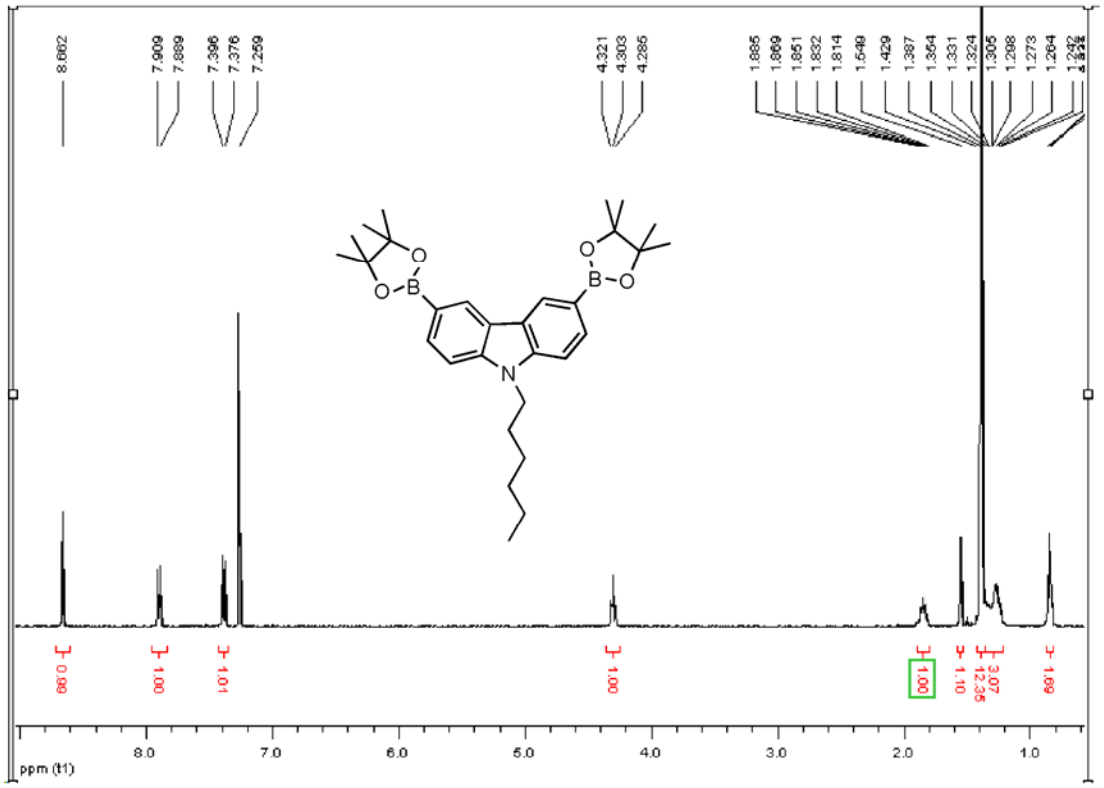


$^{13}$C NMR ($CDCl_3$, 400 MHz) spectrum of **M2**

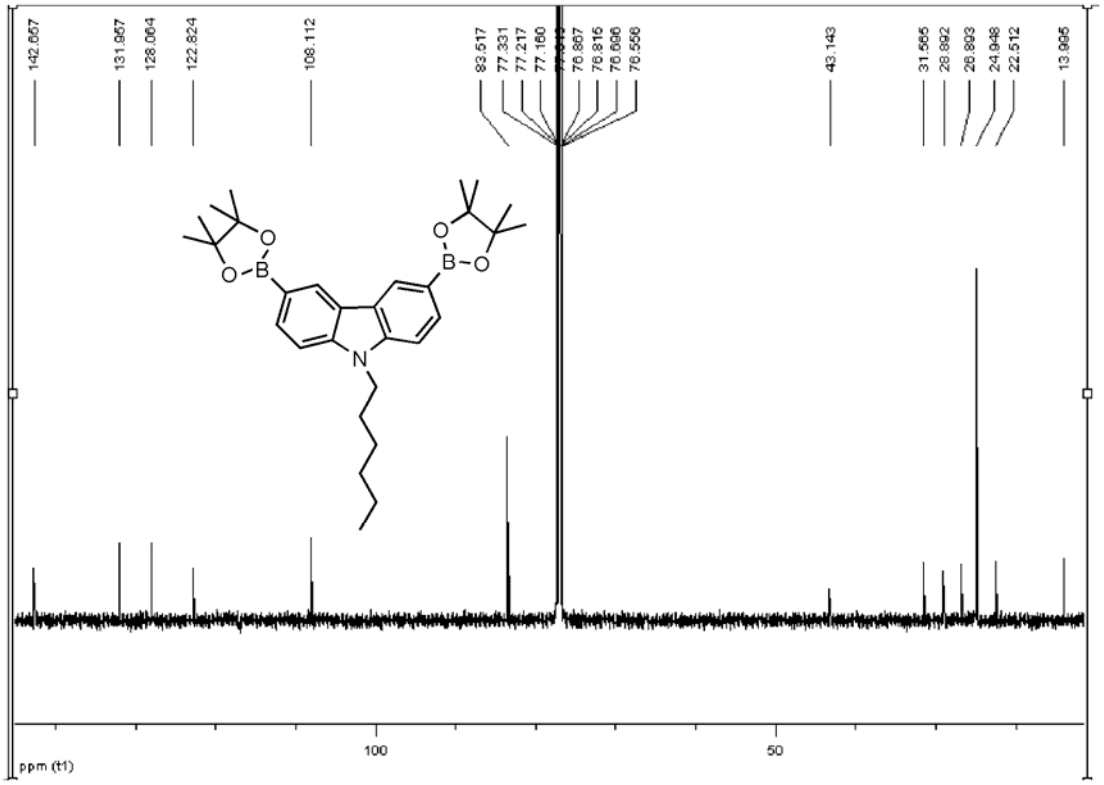

$^1$H NMR ($CDCl_3$, 400 MHz) spectrum of **P1**

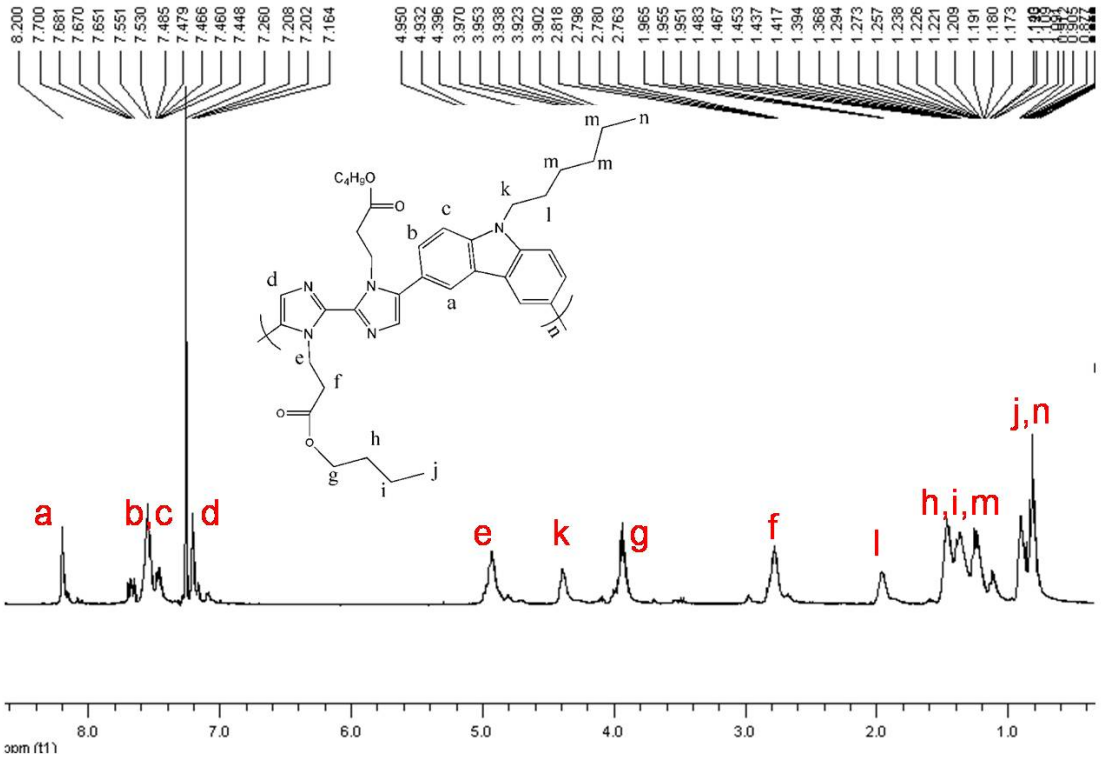


$^1$H NMR ($CDCl_3$, 400 MHz) spectrum of **P2**

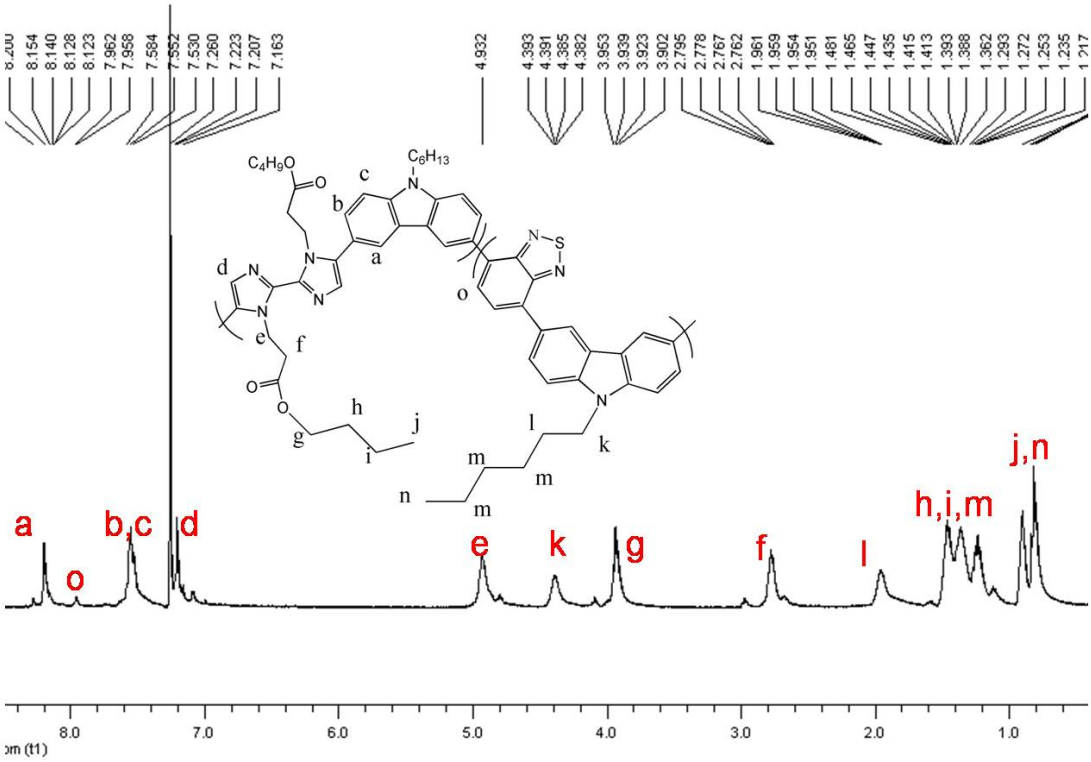

## 8. FTIR Data

FTIR spectrum of **P1**

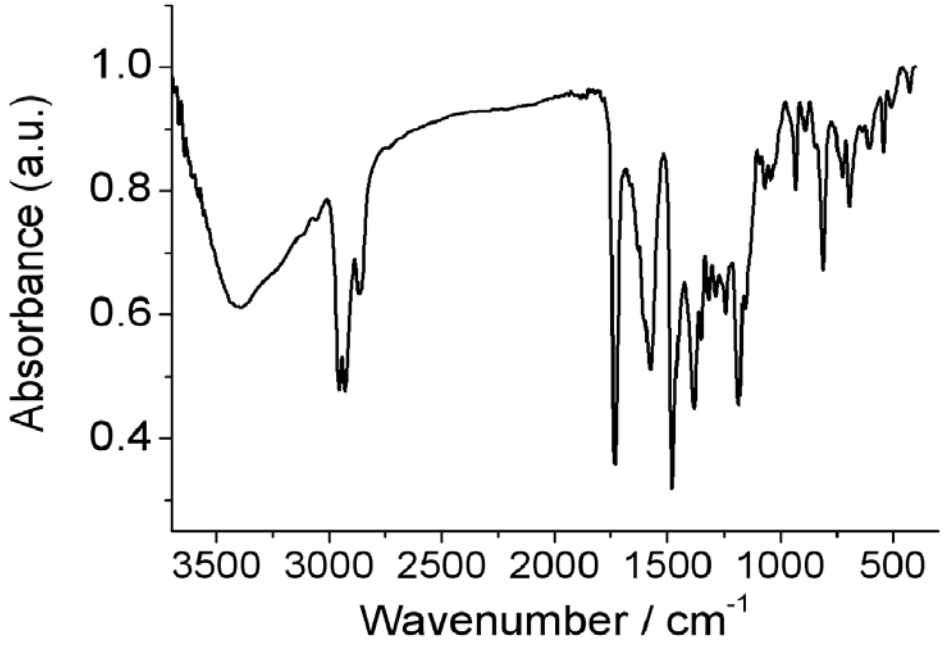


FTIR spectrum of **P2**